

Article

Nitrogen-Driven Changes in Metabolic Profile Modulate Photosynthetic Performance and Antioxidant Defense of *Amaranthus cruentus*

Enrique Ostría-Gallardo^{1,*}, Valentina Cabrera¹, Estrella Zúñiga-Contreras², José Ortiz¹, León Bravo³, Teodoro Coba de La Peña², Jaime G. Cuevas² and Luisa Bascuñán-Godoy¹

¹ Laboratorio de Fisiología Vegetal, Departamento de Botánica, Facultad de Cs. Naturales y Oceanográficas, Universidad de Concepción, Concepción 4030000, Chile

² Centro de Estudios Avanzados en Zonas Áridas, CEAZA, La Serena 1700000, Chile

³ Laboratorio de Fisiología y Biología Molecular Vegetal, Instituto de Agroindustria, Departamento de Ciencias Agronómicas y Recursos Naturales, Facultad de Ciencias Agropecuarias y Medioambiente, Universidad de La Frontera, Temuco 4780000, Chile

* Correspondence: eostria@udec.cl; Tel.: +56-41-2661032

How To Cite: Ostría-Gallardo E, Cabrera V, Zúñiga-Contreras E, Ortiz J, Bravo L, de La Peña TC, Cuevas J, & Bascuñán-Godoy L. (2025). Nitrogen-driven changes in metabolic profile modulate photosynthetic performance and antioxidant defense of *Amaranthus cruentus*. *Plant Ecophysiology*, 1(1), 4. <https://doi.org/10.53941/plantecophys.2025.100004>.

Received: 10 August 2024

Revised: 6 March 2025

Accepted: 12 March 2025

Published: 14 March 2025

Academic Editor:
Jaume Flexas Sans

Abstract: Nitrogen is crucial for plant development and crop production. *Amaranthus cruentus*, a C₄ species, has been pointed out as a high-nutritious and stress resilient crop. Here we studied the effects of sufficient and low nitrogen supplementation on the photosynthetic efficiency and metabolic responses of *A. cruentus*. Photochemical parameters from dark-adapted and transient chlorophyll fluorescence measurements, antioxidant enzymes activity, and metabolomic analysis, were evaluated to depict the impact of nitrogen availability. Photochemical parameters showed a significant decrease compared to those from gas exchange. The antioxidant enzymes activity revealed variations among treatments, being important at low nitrogen availability. At the metabolic level, there is a significant accumulation of L-glutamine, aromatic amino acids and ascorbic acid in *A. cruentus* with sufficient nitrogen. At low nitrogen, the metabolic profile of *A. cruentus* suggests stabilization of membrane structure and efficient use of available nitrogen by accumulating L-glutamic acid. The differential accumulation of L-glutamine and L-glutamic acid reflects an adaptive strategy for maintaining nitrogen. Nitrogen-rich conditions, the plant stores excess nitrogen as L-glutamine, while in deficiency, it utilizes L-glutamic acid for essential metabolic functions. Overall, *A. cruentus* activates a coordinated metabolic strategy under LN to optimize nitrogen use. This includes effective ROS detoxification via both enzymatic and non-enzymatic antioxidants, structural reinforcement through membrane-stabilizing lipids, and efficient nitrogen storage and redistribution to meet metabolic demands during nitrogen limitation.

Keywords: nitrogen supplementation; chlorophyll fluorescence; gas exchange; antioxidant activity; metabolic profiling

1. Introduction

Nitrogen is an essential component for plant growth, development, and productivity. In fact, besides water, among the environmental factors affecting plant productivity, nitrogen is the one that most limits productivity, especially in crops (Plett et al., 2020). Nitrogen influences photosynthetic efficiency as a fundamental component of chlorophyll and essential enzymes, such as RuBisCO. Hence, a deficit of nitrogen or decreased availability has a profound impact on the primary productivity of ecosystems and agricultural systems.

Nitrogen supplementation promotes biochemical adjustments in plants, leading to improved metabolic activity, even under suboptimal environmental conditions, such as drought stress (Tariq et al., 2019). Nitrogenated metabolites not only serve as building blocks for protein synthesis but also contribute to essential physiological processes and signaling pathways, enhancing plant resilience to stress (Sadak & Ramadan, 2021). Nevertheless, the level of nitrogen supply, i.e., high, moderate, or low, determines the degree of tolerance or sensitivity against abiotic stresses, such as drought (Song et al.,



2019a). For example, nitrogen supplementation in drought-stressed soybean plants increased its yield (Purcell & King, 1996), although in excess produced negative effects on water use efficiency and photosynthesis, affecting its drought tolerance response (Sun, Gao, & Lu, 2007). Also, several studies indicate that optimal nitrogen supply has a positive impact on photochemical parameters while limited nitrogen availability significantly reduces photochemical efficiency in crops such as maize, wheat, oat, rice, and tomato (Wu et al., 2019a; Song et al., 2019b; Peng et al., 2021; Li et al., 2023).

Plant responses to nitrogen availability are complex and usually species-specific (Brueck, 2008; Ren et al., 2017). *Amaranthus cruentus* L., a C₄ plant commonly known as grain amaranth, exhibits significant potential as a climate-smart crop owing to its adaptability to diverse climates and soils (Netshimbupfe et al., 2022). *A. cruentus* possesses a high nutritional value, particularly in terms of protein content, essential amino acids, and micronutrients, making it a valuable resource for combating malnutrition and enhancing food security (Cechin et al., 2022). The effect of sources and doses of nitrogen on growth, gas exchange, and some biochemical traits such as pigments, proline, and phenolic content have been reported for *A. cruentus* (Cechin et al., 2022; Zubillaga et al., 2019; Cechin & Valquilha, 2019). Nevertheless, we are still far from understanding the interplay of nitrogen availability and metabolic pathways and their impact on the photosynthetic performance of *A. cruentus*.

Given the key structural and functional role of nitrogen on primary and secondary metabolism and photosynthetic-related processes, we postulate that low nitrogen availability induces metabolic shifts towards an efficient distribution of nitrogen to sustain photosynthesis. The analyses of key physiological parameters and metabolomics provide novel insights into how nitrogen availability impacts the photochemical yield, antioxidant protection, and differential accumulation of metabolites in *A. cruentus*.

2. Materials and Methods

2.1. Plant material and experimental design

The genotype utilized in the experimental setup was *Amaranthus cruentus* Diaguaitas (ACR40). Seeds were obtained from the National Seed Bank collection of the Instituto de Investigaciones Agropecuarias (INIA-Intihuasi) located at Vicuña, Chile (19 J 336895.75 m E 6675781.94 S). At a nursery garden located at the University of Concepción, plants of *A. cruentus* were grown from seeds sown directly on 5 kg of dry soil in 11 L pots (22 cm height by 28 cm diameter; two plants per pot). The soil in the pot contained a mixture of 80% washed sand and 20% peat and a basal fertilization with 4 g of 6 M Basacote Plus Compo Expert (16% N, 3.5% P, 10% K, 1.2% Mg, 5% S, and micronutrients) according to Cifuentes et al. (2023). Pots were irrigated at field capacity (FC) by monitoring the soil water content using a time-domain reflectometer soil moisture meter TDR350 (FieldScout Spectrum Technologies,

Inc., Aurora, IL, USA), according to Ostria-Gallardo et al. (2020). The frequency of irrigation was every two days.

The experimental design consisted of evaluating two levels of nitrogen availability as follows: sufficient nitrogen (C), low nitrogen (LN). Each treatment contained 24 pots, each pot containing one plant. For nitrogen treatments, plants with the fourth pair of true leaves were supplemented with urea (CH₄N₂O) to reach both N-level treatments: sufficient nitrogen (C; 0.6 g of N per pot) and low nitrogen soils (LN; 0.30 g of N per pot). These concentrations were used to determine the optimal and insufficient N fertilization levels. We opted for urea as nitrogen source due to its lower risk of causing salt injury, compared to ammonium nitrate or ammonium sulfate, and because it is the most widely used nitrogen fertilizer worldwide. Sampling and measurements were carried out 30 days after the application of the nitrogen doses.

2.2. Quantification of total leaf nitrogen, soluble sugars and starch content

The total leaf nitrogen content (%) was determined using the Kjeldahl method, following the procedure described in <https://prometheusprotocols.net/>. Briefly, 0.5 g of dried and finely ground leaf samples were placed in a digestion tube with 5 mL concentrated H₂SO₄ and a catalyst mixture composed of 10 g K₂SO₄ and 0.5 g CuSO₄. The samples were subjected to digestion and further titration with 0.1 N HCl until the endpoint was reached, indicated by a color change from green to pink. The total nitrogen content was calculated as: Total Nitrogen (%) = (V × N × 1.4)/W, where V is the volume (mL) of HCl used in titration, N is the normality of the HCl solution, 1.4 is the conversion factor for nitrogen in the Kjendahl method, and W is the weight (g) of the sample.

Soluble sugars were extracted from 50 mg fresh leaf material using 80% ethanol, according to Chow & Landhäusser (2004). Following extraction, the extracts were centrifuged at 2500 rpm for 5 min at 4 °C. The total soluble sugar content was determined using the anthrone reagent at 490 nm. Starch was extracted from the residue of the extracts using a boiling solution of 3% perchloric acid. Thus, starch is hydrolyzed to glucose. Glucose in the hydrolyzed extract was colorimetrically determined using anthrone reagents at 525 nm.

2.3. Chlorophyll fluorescence and gas exchange

Chlorophyll fluorescence measurements were conducted with an OS30p+ fluorometer (Opti-Science, Inc., Hudson, USA) to determine the dark-adapted parameters informing quantum yield (protocol 1) and transient OJIP curves (protocol 2). For protocol 1, leaves were dark-adapted overnight before measurements. Leaves were clamped with leaf clips and the probe of the fluorometer was inserted in each leaf clip. The actinic light used was 900 μmol quanta m⁻² s⁻¹. The maximum quantum yield of PSII (F_v/F_m), the maximum primary yield of PSII (F_v/F_o), and the actual quantum yield (ΦPSII) were calculated as described in Maxwell & Johnson (2000), and Kramer et al. (2004). For transient OJIP tests (protocol 2), the

actinic light used was 3500 μmol and 80% modulation of light intensity. Fluorescence parameters and the log last trace were recorded and double normalized by F_0 and F_m values for further analysis of the OJIP parameters (Pollastri et al., 2022).

Leaf gas exchange measurements were made to estimate the effect of nitrogen supply on carbon assimilation (A_{sat}), stomatal conductance (g_s), and the electron transport rate (ETR) and the intrinsic water use efficiency (iWUE) using a gas exchange system (LI-6400, Li-Cor Inc., Lincoln, USA) with a 2 cm^2 leaf chamber of with an LED light source (LI-6400-40). Leaves were carefully placed in the sensor head, ensuring contact with the leaf thermocouple. Light-saturated CO_2 assimilation (A_{sat}), stomatal conductance (g_s), and apparent transpiration rate (E) were measured in 12 individuals per species from 9:00 to 13:00. Gas exchange parameters were recorded 10 min after clamping the leaf. Leaf chamber conditions were set at 400 $\mu\text{mol mol}^{-1}$ of CO_2 , 1200 $\mu\text{mol photons m}^{-2} \text{ s}^{-1}$ (90:10% red: blue light), 60–65% relative humidity, and 25 °C block temperature. The intrinsic water use efficiency (iWUE) was calculated as the ratio of photosynthesis (A_{sat}) over stomatal conductance (g_s). To verify both proper equipment performance and status of control plants, the ratio of electron transport rate to assimilation (ETR/A) was evaluated according to Perera-Castro & Flexas, (2023).

2.4. Antioxidant activity

The antioxidant enzyme assays i.e., ascorbate peroxidase (E.C. 1.11.1.11, APX), glutathione reductase (E.C. 1.6.4.2, GR), superoxide dismutase (E.C. 1.15.1.1, SOD) and Peroxidase (POD), activities were determined by the methods described in Palma et al, (2014). Briefly, 1g fresh leaves was ground with liquid nitrogen and homogenized with 2 mL of 50 mM potassium phosphate buffer (20% w/v polyvinylpyrrolidone, 0.1 mM EDTA, 10 mM β -mercaptoethanol, pH 7.8). The homogenate was centrifuged at 13,000 \times g 20 min at 4 °C, and the supernatant was used for determinations of enzyme activity and total protein content by Bradford (1976). Ascorbate peroxidase uses ascorbate as an electron donor and was evaluated spectrophotometrically by the decrease in absorbance at 290 nm after 10 min on a reaction mix of 50 mM Tris-HCl pH 7.8, 0.4 mM ascorbate, and 0.3 mM H_2O_2 , the last two added moments before starting the measurements. Superoxide dismutase catalyzes the dismutation of superoxide radicals into oxygen and hydrogen peroxide and was determined at 560 nm by the inhibition of the photochemical reduction of nitroblue tetrazolium chloride (NBT). The activity is expressed as unit $\text{min}^{-1} \text{ mg}^{-1}$ protein, where one unit of SOD is equal to the amount of enzyme that inhibits 50% of NBT photoreduction. Peroxidase (POD) was determined at 470 nm by monitoring the oxidation of guaiacol. The reaction mix contained 200 mM sodium phosphate buffer pH 5.8, 7.2 mM guaiacol, and 11.8 mM H_2O_2 as cofactor. Glutathione reductase (GR) activity maintains the reduced state of glutathione and was evaluated at 340 nm by measuring the decrease in absorbance due the NADPH oxidation. For this, the reaction mix contained 0.2 mM NADPH, 0.1 mM HEPES-NaOH, 3 mM MgCl_2 , 1 mM EDTA, and 0.25 mM oxidized glutathione.

2.5. Metabolomic analysis

A total of 32 leaves from individuals of the different treatments were collected and freeze-dried. Samples were sent to the Sequencing and Omics Technologies Unit at Pontificia Universidad Católica de Chile (Secuenciación y Tecnologías ómicas–Facultad de Ciencias Biológicas (uc.cl)) for samples preparation and chromatography. Briefly, 3 μL of sample was injected on a Compact QTOF MS + Elute UHPLC spectrometer. Separation was done by using a Kinetex C18 column. Raw data was preprocessed with MS-DIAL for m/z peak detection, noise reduction, retention time alignment, and peak integration. Further, the m/z and MS/MS spectra were matched to MassBank database for annotation. For statistical analysis, we used those metabolites that fall within confidence level 2 (Summer et al., 2007). Preliminary data analysis was performed in the software Metaboscape v4.0. The relative quantities of metabolites from both positive and negative ionization modes were merged and imported into MetaboAnalyst v6.0 software (Pang et al., 2024). Data was filtered by interquartile ranges, log10 transformed, scaled by mean-center, and normalized by sum for further analyses according to Cifuentes et al, (2023).

2.6. Data analysis

Data were checked for normality assumptions and variance homoscedasticity with the InfoStat software. Accordingly, the parametric two-way ANOVA or non-parametric Kruskal–Wallis analyses were used to compare means between treatments. When significant differences were found, we used post hoc tests with Tukey or pairwise comparisons ($p \leq 0.05$), depending on the parametric or non-parametric nature of the data. For chlorophyll *a* fluorescence and gas exchange data we calculate the percentage change to assess the level of increase or decrease in the parameters of control (C) versus low nitrogen (LN). The percentage change was calculated by the following formula:

$$\Delta\% = ((M2 - M1)/M1) \times 100$$

where M1 is the mean value of a parameter in C, and M2 is the mean value of the parameter in LN.

For untargeted metabolomics, scaled and normalized data were analyzed for differential accumulation differences, chemometric, and cluster analyses. For these analyses, metabolites were considered significantly accumulated at $p < 0.05$. A Sparse Partial Least Square Discriminant Analysis was used to determine specific metabolites associated with the different treatments. For cluster analysis, the interquartile ranges of normalized data were used to apply the Ward's hierarchical cluster analysis and the Euclidean distance to evaluate the metabolite accumulation patterns regarding nitrogen supply and water availability. Finally, we used the Pathway analysis tool of Metaboanalyst 6.0 (Pang et al., 2024) to predict the impact of differentially accumulated metabolites in specific metabolic pathways.

3. Results

3.1. Total leaf nitrogen, soluble sugars and starch

Leaf nitrogen content varied significantly depending on nitrogen supply. Specifically, the decrease of total nitrogen was 51.52% from C to LN ($p = 0.0013$; Table 1). The metabolic partitioning of carbohydrates, specifically total soluble sugars (TSS) and starch, showed non-significant changes (Table 1), suggesting a steady carbohydrate metabolism under the tested conditions.

3.2. Nitrogen availability affects significantly the photochemical response of *A. cruentus*

Deeper insights into the photosynthetic process of *A. cruentus* under varying nitrogen supply were gained from transient and dark adapted chlorophyll fluorescence

measurements. The analysis of chlorophyll *a* transient curve (OJIP) provided insights on the effect of nitrogen availability over PSII efficiency and, consequently, plant photosynthetic capacity (Table 2). All fluorescence-derived parameters showed significant differences (Table 2). The sufficient nitrogen treatment (C) significantly outperformed the nitrogen deficit (LN) treatment, exhibiting higher values in the maximum quantum yield of PSII (F_v/F_m), maximum primary yield of PSII (F_v/F_0), Performance Index (PI) and the amplitude of relative variable fluorescence in the I-P rise (ΔVIP). Except for A_{sat} , nitrogen availability has no significant effects over gas exchange parameters (Table 2). Additionally, A_{sat} showed a significant decrease of 23.19% from C to LN, whereas the other gas exchange parameters showed non-significant changes. However, the largest percentage decrease between C to LN was observed in chlorophyll *a* parameters, except for V_J which showed an increase of 36% (Table 2).

Table 1. ANOVA results for mean values of total leaf nitrogen (in percentage of dry mass), total soluble sugars, and starch content of *A. cruentus* leaves ($n = 3$ leaves per treatment). Acronyms denote treatments as follows: sufficient nitrogen (C), low nitrogen (LN). Asterisk (*) indicates significant differences at $p < 0.05$.

Treatment	Total Leaf Nitrogen (%)	Total Soluble Sugars (mg g ⁻¹)	Starch (mg g ⁻¹)
C	2.95 *	2.41 ± 0.595	84.06 ± 10.840
LN	1.43	2.08 ± 0.301	72.58 ± 20.56

Table 2. ANOVA and percentage change ($\Delta\%$) of chlorophyll *a* fluorescence and gas exchange parameters under control (C) and low nitrogen (LN) treatments. Single asterisk (*) denotes significant effects at $p < 0.05$, and double asterisk (**) denotes significant effects at $p < 0.001$. Arrows indicate the direction of percentage change, with a decrease (↓) or increase (↑) in parameters when comparing C to LN.

Chlorophyll <i>a</i> Parameters			
	C (Mean ± S.E.)	LN (Mean ± S.E.)	$\Delta\%$
F_v/F_0	2.91 ± 0.14 **	2.17 ± 0.09	25.43 (↓)
F_v/F_m	0.79 ± 0.01 **	0.68 ± 0.01	13.92 (↓)
V_J	0.45 ± 0.03 *	0.61 ± 0.04	35.56 (↑)
PI	2.41 ± 0.49 *	0.65 ± 0.12	73.03 (↓)
ΔVIP	0.27 ± 0.01 **	0.20 ± 0.01	25.93 (↓)
Gas Exchange Parameters			
	C (Mean ± S.E.)	LN (Mean ± S.E.)	$\Delta\%$
A_{sat}	22.03 ± 0.71 *	16.92 ± 1.86	23.19 (↓)
g_s	0.14 ± 0.01	0.11 ± 0.01	21.43 (↓)
E	2.37 ± 0.10	2.52 ± 0.26	6.33 (↑)
$iWUE$	158.57 ± 9.85	150.74 ± 9.35	4.94 (↓)
ETR	138.42 ± 4.62	127.96 ± 5.03	7.56 (↓)

3.3. Performance of antioxidant enzyme activities in *A. cruentus* leaves

The activities of key antioxidant enzymes, including APX, GR, and POD exhibited significant modulation in response to variations in nitrogen supply (Figure 1). Activity of APX, crucial for scavenging hydrogen peroxide, was markedly high in the LN treatment (Figure 1A), showing an increase of 77.8% of activity compared to C.

The activity of GR and POD were significantly higher in the LN condition (Figure 1C,D), with an increase of 133% and 50%, respectively.

3.4. Metabolomic profile and differential accumulation of metabolites in *A. cruentus* under varying nitrogen supply

The metabolomic results provide a comprehensive insight into the metabolic adjustments of *A. cruentus* in response to nitrogen supply. The partial least square–discriminant analysis (PLSDA) showed a distinct clustering pattern of the treatments (Figure 2A), highlighting these metabolites that contribute the most to these patterns of clustering according to the variable importance in projection (VIP) scores (Figure 2B). L-glutamine, phenylalanine and L-norleucine were the metabolites with the highest contribution to the variability observed along Components 1 and 2 (Figure 2B). Further, we analyzed the differential accumulation of metabolites and metabolic pathways that were modulated in response to the experimental conditions (Figures 3 and 4). In Figure 3A, the heatmap illustrates patterns of metabolite accumulation across the treatments. Notably, L-glutamine, L-norleucine, phenylalanine,

L-tryptophan, and the antioxidant ascorbic acid showed elevated levels in the C condition. Furthermore, high accumulation of ferulic and coumaric acids was also detected in C.

By contrast, lower levels of metabolites such as pheophorbide, phosphatidylcholine, and phosphatidylethanolamine were observed in the C treatment. On the other hand, L-glutamic acid was elevated under low nitrogen supply (LN). Also, lipids such as lysophosphatidylcholine and 1-palmitoyl-2-oleoyl-sn-glycero-3-phosphocholine, as well as flavonoids and phenolic compounds such as rutin, ferulic acid and chlorogenic acid showed high accumulation in response to LN.

Given the differential accumulation L-glutamine and L-glutamic acid depending on nitrogen supply, i.e., high levels of L-glutamine at C, high levels of L-glutamic acid at LN, we explored

the correlations with other metabolites to get insight into the metabolic dynamic of *A. cruentus* across the different treatments (Figure 3B). Arginine and phenylalanine positively correlate with L-glutamine ($p < 0.01$, $r > 0.5$). On the other hand, L-glutamic acid correlated positively mostly with lipids, and a negative correlation was observed with aromatic amino acids and coumarins. Finally, the pathway impact analysis further elucidates the metabolic pathways significantly modulated by the treatments (Figure 4). We found that alanine, aspartate and glutamate metabolism, and nitrogen metabolism exhibit the highest impact, noting the crucial role of metabolites involved in these pathways, particularly L-glutamine and L-glutamate, for the response of *A. cruentus* to different nitrogen availability.

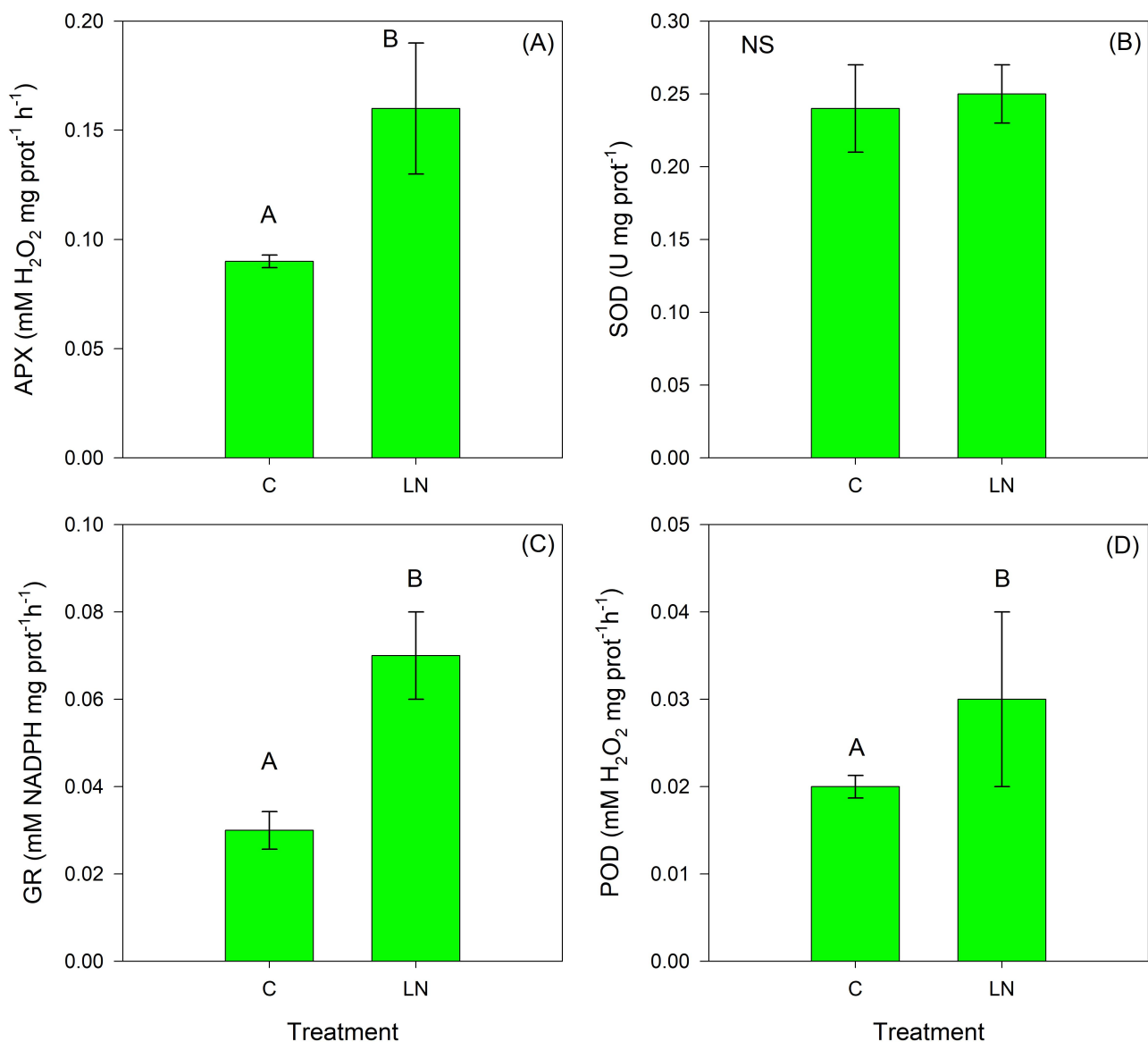


Figure 1. Effects of nitrogen supply and water availability on antioxidant enzymes. (A) ascorbate peroxidase (APX), (B) superoxide dismutase (SOD), (C) glutathione reductase (GR), and (D) peroxidase (POD). Enzyme activities were evaluated on healthy and fully expanded leaves of $n = 3$ individuals per treatment. The bars and vertical lines above the bars indicate the mean and the standard error values, respectively. Uppercase letters indicate significant differences between treatments at $p < 0.05$.

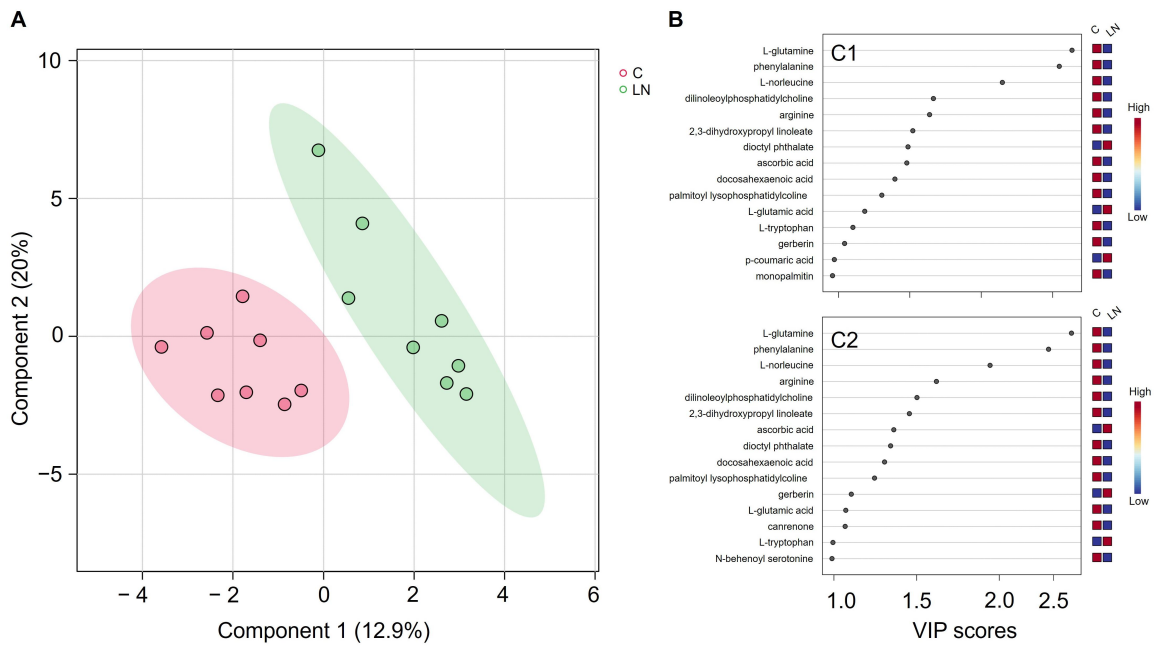


Figure 2. (A) Partial Least Square Discriminant Analysis plot (PLS-DA). The two-dimensional space shows the 95% confidence region of samples from control (C, red) and low nitrogen (LN, green) treatments. Components 1 and 2 collectively explain 32.9% of data variability between C and LN. Panel (B) shows the Variable Importance in Projection (VIP, X axis) score of metabolites (Y axis) in Components 1 and 2 (C1,C2), identifying the metabolites that contribute significantly to the variability of the data. The higher the VIP score, the higher the contribution of a metabolite in the variability of the response between C and LN. The color pallet in (B) indicates the contribution of specific metabolites that contribute most to the variability among treatments, from high (red) to low (blue) contribution.

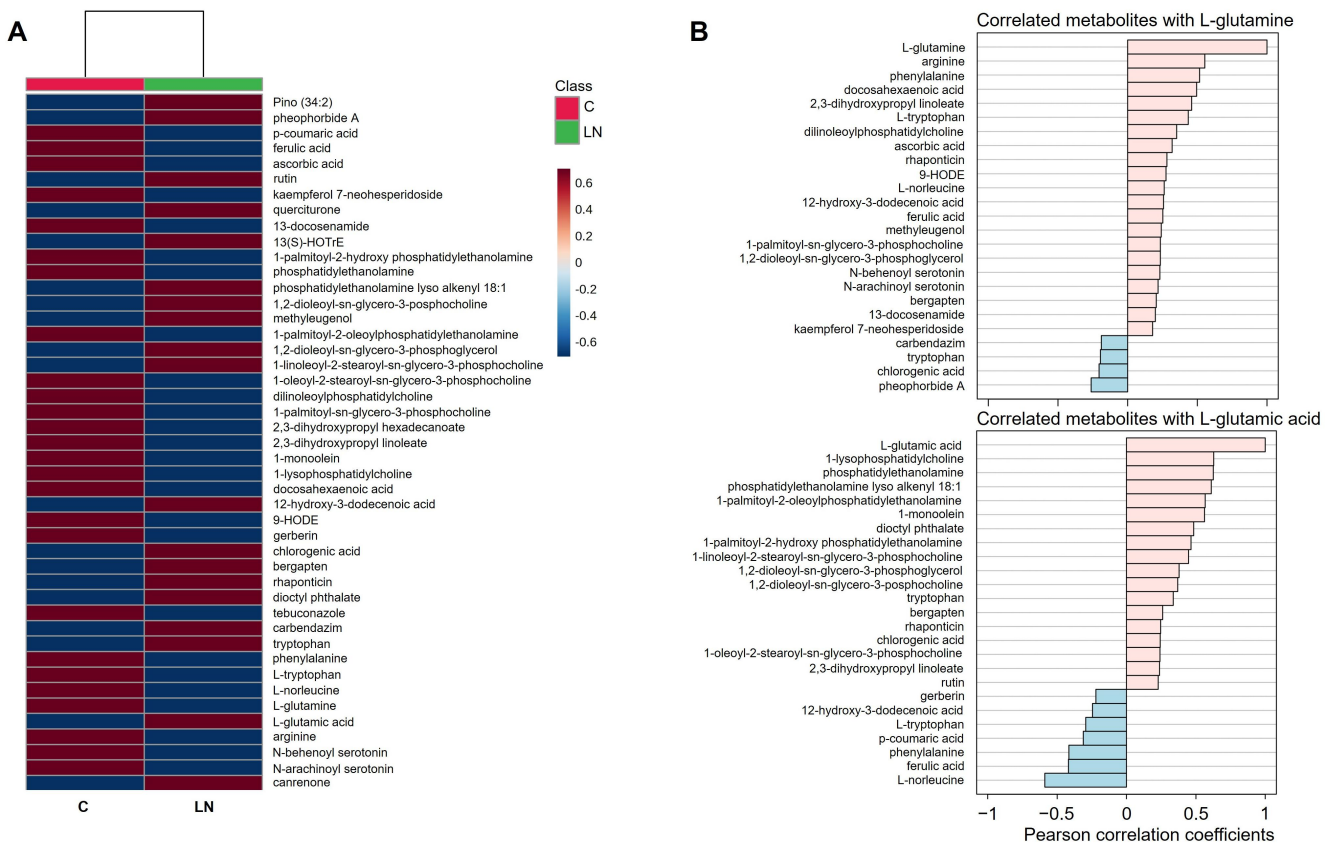


Figure 3. Heatmap for metabolome profiling data (A) showing the accumulation patterns of 47 non-repeated identified metabolites under the different treatments. The scale bar shows the normalized value for metabolite quantification from low(blue) to high (red) levels of accumulation. Panel (B) shows the Pearson correlation coefficients of L-glutamine and L-glutamic acid with the top 25 highly up-or-down accumulated metabolites in C and LN. Red and blue bars in the Pearson correlation plots denote positive and negative correlations, respectively.

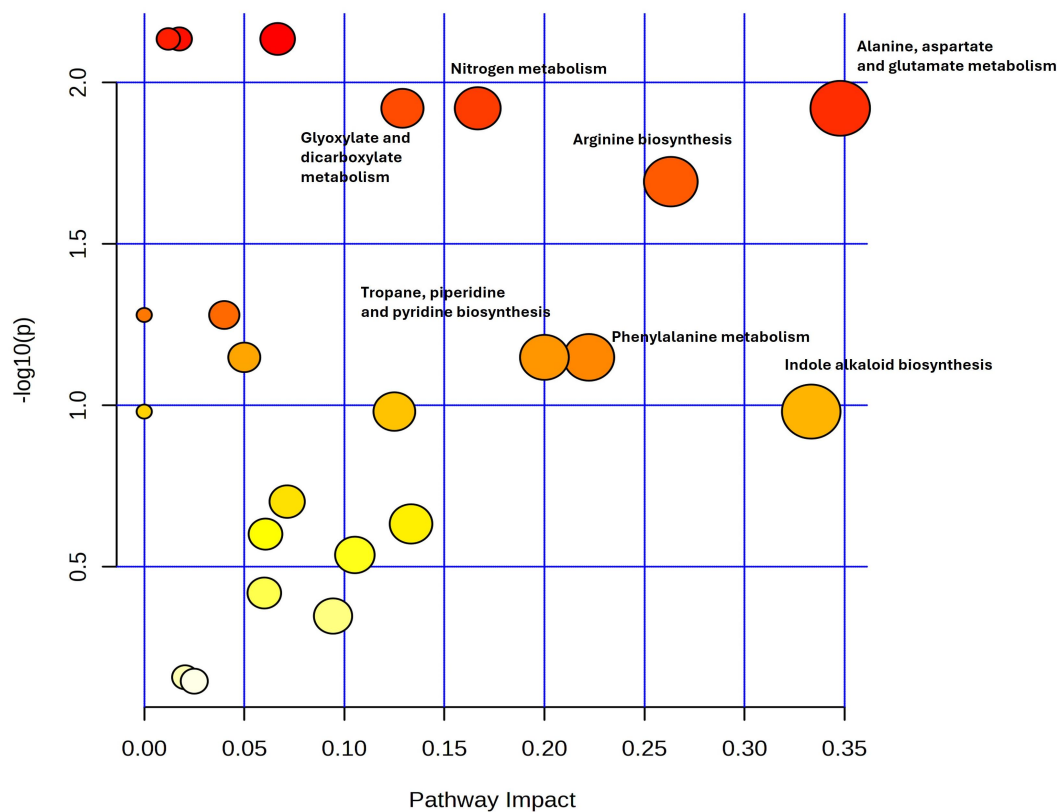


Figure 4. Pathway impact analysis based on the differential accumulation patterns of metabolites between treatments. The analysis predicts the position and roles of each metabolite within a pathway. The plot highlights those pathways that show significant alterations in response to the level of accumulation of metabolites. The size of the circles indicates the level of impact in pathways that are modulated by the treatments. The color inside the circles indicates the significance (\log_{10} of p value) of the change of metabolite levels in each metabolic pathway. Accordingly, alanine, aspartate, and glutamate metabolism, arginine biosynthesis, glyoxylate and dicarboxylate metabolism, and nitrogen metabolism pathways exhibit the highest impact of the variation of accumulation of metabolites depending on C or LN conditions.

4. Discussion

Nitrogen availability has significant effects on the total content of nitrogen in leaves (Table 1), highlighting the responsiveness of *A. cruentus* to varying nitrogen supply. Nevertheless, the leaf total soluble sugars and starch showed no significant differences despite observing a decrease under LN conditions. Although the effect of nitrogen over the content of leaf carbohydrates varies widely among species, a common response is either to increase TSS and decrease starch content or vice versa (Wu et al., 2019b; Mariem et al., 2020; Zhao et al., 2020). One possible explanation for our TSS and starch results is a stable carbon metabolism under varying nitrogen content due to the C_4 carbon concentration mechanism of amaranth. Ultimately, this would help the plant to use and invest carbon in root growth to explore soil for nitrogen acquisition while maintaining carbohydrate availability for respiratory demand in response to nitrogen deficiency (Zhao et al., 2020).

We observed a significant decrease in the photochemical efficiency of *A. cruentus* under LN, as evidenced by chlorophyll a parameters (Table 2). Further, our analysis showed that the largest percentage decrease changing from C to LN conditions was larger in the photochemical processes than in the gas exchange processes and parameters. The largest decreases were observed in the performance index (PI), while there was a large increase in the V_j parameter. The former is an indicator of the overall photosynthetic performance, while the latter typically

reflects the rate at which quinones (QA) transition from the reduced state (QA^-) back to the oxidized state (QA). High values of V_j often suggest optimal electron transference within PSII. Counterintuitively, V_j increases under LN. Under certain stress conditions, such as high light intensity or temperature stress, V_j can increase (Serôdio, Schmidt, & Franenbach, 2017; Marečková, Barták, & Hájek, 2019). The increase under stress conditions has been proposed as a protective mechanism, where PSII maintains a high turnover rate of electrons to minimize damage by excess excitation energy.

Regarding gas exchange, a decrease of nitrogen supply affects mainly to A_{sat} and g_s , yet has negligible impact on transpiration, ETR and $iWUE$. Sufficient nitrogen supply has been shown to enhance WUE under certain stress conditions (Plett et al., 2020; Sadras & Rodriguez, 2010). A comprehensive meta-analysis highlights that the beneficial impacts of nitrogen on WUE predominantly result from improved physiological processes rather than stomatal dynamics (Brueck, 2008). In our study, physiological adjustments under LN appear to prioritize efficient water management, enabling *A. cruentus* to maintain stable g_s and transpiration rates. Low nitrogen typically decreases photosynthetic enzyme levels, particularly RuBisCO, limiting carbon assimilation. Consequently, C_4 metabolism, as the CO_2 -concentrating mechanism, allows *A. cruentus* to maintain internal CO_2 levels in bundle-sheath cells, contributing a stable $iWUE$.

The interplay between low nitrogen supply and the antioxidant enzyme system resulted in increased activity of key antioxidant enzymes, pivotal for mitigating oxidative stress by scavenging reactive oxygen species (ROS) and maintaining cellular redox homeostasis (Ding et al., 2020). Elevated activity of enzymes such as glutathione reductase (GR), ascorbate peroxidase (APX), and peroxidase (POD) under LN not only highlights the critical role of nitrogen in sustaining redox balance but also suggests mechanisms that support photochemical stability (Hamada et al., 2023). In particular, the enhanced activity of GR under LN contributes to maintaining the redox state of ascorbate and glutathione pools, which are essential for protecting photosystems from oxidative damage. Additionally, there appears to be a feedback mechanism between photochemical efficiency and ROS regulation. Reductions in nitrogen availability impair photochemical efficiency, which may lead to an increase in ROS formation. The elevated antioxidant enzyme activity under LN seems to counterbalance this potential rise in ROS, protecting photosystem II (PSII), particularly at the quinone level. Consequently, these findings suggest that the increase in antioxidant enzyme activity under LN is not only a direct response to redox imbalances but also an integral part of a broader protective mechanism when low nitrogen availability comprises the functioning of photosystems as observed in the photochemical results for *A. cruentus*.

Our metabolomic analysis reveals distinct patterns of metabolite accumulation under varying nitrogen conditions, indicating that nitrogen availability significantly shapes the metabolic responses in *A. cruentus*. Under sufficient nitrogen, metabolites associated with nitrogen storage and cellular protection, such as L-glutamine, ascorbic acid, and aromatic amino acids, were present in elevated levels. Notably, L-glutamine and L-norleucine accumulated abundantly, reflecting their roles in nitrogen assimilation and redistribution, which are essential for maintaining cellular functions and supporting nitrogen storage mechanisms. Under LN conditions, there are metabolic shifts, particularly among nitrogenous compounds, antioxidants, and structural stabilizers, each playing specific roles in cellular stability and stress response. Elevated levels of L-glutamic acid under LN suggest a metabolic adjustment towards efficient nitrogen use, mobilizing scarce nitrogen towards critical processes such as amino acid synthesis, nitrogen transport, and the functioning of citric acid cycle (The, Snyder, & Tegeder, 2021). This shift appears to support sustained metabolic activity under limited nitrogen, with L-glutamic acid also serving as a precursor to glutathione, thereby linking it to the observed increase in GR activity in LN. These nitrogenous metabolites primarily impact the phenylpropanoid and arginine biosynthetic pathways and broader nitrogen metabolism (Figure 4), suggesting that *A. cruentus* activates a coordinated metabolic strategy under LN to optimize nitrogen use. This includes effective ROS detoxification via both enzymatic and non-enzymatic antioxidants, structural reinforcement through membrane-stabilizing lipids, and efficient nitrogen storage and redistribution to meet metabolic demands during nitrogen limitation.

Antioxidant compounds, including rutin, quercitrone, and chlorogenic acid, were notably higher under LN. These metabolites likely enhance the oxidative stress defenses, as chlorogenic acid is known to activate antioxidant enzymes such as POD (Rice-Evans, Miller, & Paganga, 1997; Agati et al., 2020). The increase in these flavonoids and phenolic compounds suggests a reinforced non-enzymatic antioxidant response, complementing the enzymatic antioxidant system to provide ROS detoxification under nitrogen deficiency. This dual antioxidant strategy appears vital for maintaining cellular redox balance. Furthermore, the accumulation of L-glutamic acid correlates positively with structural stabilizers, such as lipid compounds like palmitoyl phosphoethanolamine (palmitoyl-PE; Figure 3B). This lipid likely contributes to membrane stabilization under oxidative stress, supporting cell integrity in the face of nitrogen deficiency (Cechin et al., 2022; Colin & Jaillais, 2020). The observed coordination between L-glutamic acid and structural lipids suggests that LN-induced oxidative stress may trigger a reorganization of membrane composition, with glutamic acid playing a key role in fortifying cellular structures through lipid interactions.

Finally, the dynamic regulation of L-glutamine (gln) and L-glutamic acid (glu) levels highlight their central roles in metabolic pathways modulation of *A. cruentus* in response to nitrogen availability. L-glutamine and L-glutamic acid have been widely reported as key for transport and metabolic use in plants, respectively (Watanabe et al., 2013; Lee, Liao, & Hsieh, 2023). Beyond their absolute concentration, the gln/glu ratio can inform about metabolic shifts regarding nitrogen use. Comparing the gln/glu ratio in *A. cruentus*, the control treatment (C) showed a significantly higher value ($p = 0.03$) than in LN (Figure S1). High values of gln/glu indicate that the plant has sufficient nitrogen for storage and transport, whereas a low ratio indicates that the plant is optimizing the use of the available nitrogen to sustain metabolic functions. Given the crucial roles of gln and glu in growth, development, and stress response (Lee, Liao, & Hsieh, 2023), the L-glutamine and L-glutamic acid metabolism and the enzymatic control over their levels would play a crucial physiological role in *A. cruentus* to cope with low nitrogen availability.

5. Conclusions

Our study elucidates the critical role of nitrogen availability in the physiological and metabolic responses of *A. cruentus*. Under nitrogen deficit, photochemistry is significantly more affected than gas exchange, with enhanced antioxidant defenses indicating elevated oxidative stress that compromises photosystem integrity and reduce photochemical yield. Simultaneously, nitrogen scarcity leads to decreased CO₂ assimilation, although partial stomatal closure occurs without impacting transpiration or iWUE.

The differential accumulation of L-glutamine and L-glutamic acid reflects an adaptive strategy for maintaining and using nitrogen. Under nitrogen-rich conditions, the plant stores excess nitrogen as L-glutamine, while in deficiency, it utilizes

L-glutamic acid to optimize the use of the available nitrogen for essential metabolic functions.

Understanding nitrogen dynamics in *A. cruentus* offers valuable insights for managing nitrogen in related C₄ crops. Future research should focus on breeding strategies to enhance nitrogen use efficiency and resilience in C₄ species, aiming to develop cultivars that can withstand nitrogen limitation. This study underscores the importance of precise nitrogen management for enhancing plant resilience and productivity under varying environmental conditions.

Supplementary Materials

The additional data and information can be downloaded at: <https://www.scilitp.com/journals/PlantEcophys/2025/1/448/s1>.

Author Contributions

E.O.-G. and L.B.-G. designed the research. E.O.-G., V.C., E.Z.-C., and J.O. performed the research. E.O.-G., J.O., L.B., T.C.d.L.P., J.C., and L.B.-G. discussed and interpreted the data. EO-G drafted the first version, and all authors contributed to the final writing, review, and editing of the manuscript.

Funding

Agencia Nacional de Investigación y Desarrollo (ANID), Fondecyt Iniciación Grant N°11201086; Agencia Nacional de

References

- Agati G, Brunetti C, Fini A, Gori A, Guidi L, Landi M, & Tattini M. (2020). Are flavonoids effective antioxidants in plants? Twenty years of our investigation. *Antioxidants*, 9(11), 1098. <https://doi.org/10.3390/antiox9111098>
- Bradford MM. (1976). A rapid and sensitive method for the quantitation of microgram quantities of protein utilizing the principle of protein dye binding. *Analytical Biochemistry*, 72(1–2), 248–254. [https://doi.org/10.1016/0003-2697\(76\)90527-3](https://doi.org/10.1016/0003-2697(76)90527-3)
- Brucek H. (2008). Effect of nitrogen supply on water-use efficiency of higher plants. *Plant Nutrition and Soil Science*, 171(2), 210–219. <https://doi.org/10.1002/jpln.200700080>
- Cechin I, & Valquiha ÉM. (2019). Nitrogen effect on gas exchange characteristics, dry matter production and nitrate accumulation of *Amaranthus cruentus* L. *Brazilian Journal of Botany*, 42, 373–381. <https://doi.org/10.1007/s40415-019-00542-1>
- Cechin I, da Silva LP, Ferreira ET, Barrochelo SC, de Melo FPD SR, Dokkedal AL, & Saldanha LL. (2022). Physiological responses of *Amaranthus cruentus* L. to drought stress under sufficient- and deficient-nitrogen conditions. *PLoS ONE*, 17(7), e0270849. <https://doi.org/10.1371/journal.pone.0270849>
- Chow PS, & Landhäusser SM. (2004). A method for routine measurements of total sugar and starch content in woody plant tissues. *Tree Physiology*, 24(10), 1129–1136. <https://doi.org/10.1093/treephys/24.10.1129>
- Cifuentes L, González M, Pinto-Irish K, Álvarez R, Coba de la Peña T, Ostria-Gallardo E, Franck N, Fischer S, Barros G, Castro C, Ortiz J, Sanhueza C, Del-Saz NF, Bascunan-Godoy L, & Castro PA. (2023). Metabolic imprint induced by seed halo-priming promotes a differential physiological performance in two contrasting quinoa ecotypes. *Frontiers in Plant Science*, 13, 1034788. <https://doi.org/10.3389/fpls.2022.1034788>
- Colin LA, & Jaillais Y. (2020). Phospholipids across scales: Lipid patterns and plant development. *Current Opinion in Plant Biology*, 53, 1–9. <https://doi.org/10.1016/j.pbi.2019.08.007>
- Ding H, Wang B, Han Y, & Li S. (2020). The pivotal function of dehydroascorbate reductase in glutathione homeostasis in plants. *Journal of Experimental Botany*, 71(12), 3405–3416. <https://doi.org/10.1093/jxb/eraa107>
- Hamada, A., Tanaka, Y., Ishikawa, T., & Maruta, T. (2023). Chloroplast dehydroascorbate reductase and glutathione cooperatively determine the capacity for ascorbate accumulation under photooxidative stress conditions. *The Plant journal: for cell and molecular biology*. <https://doi.org/10.1111/tbj.16117>
- Kramer DM, Johnson G, Kिरrats O, & Edwards GE. (2004). New fluorescence parameters for the determination of QA redox state and excitation energy fluxes. *Photosynthesis Research*, 79(2), 209–218. <https://doi.org/10.1023/B:PRES.0000015391.99477.0d>
- Lee K, Liao H, & Hsieh M. (2023). Glutamine metabolism, sensing, and signaling in plants. *Plant & Cell Physiology*, 64(12), 1466–1481. <https://doi.org/10.1093/pcp/pcad054>
- Li C, Yang Z, Zhang C, Luo J, Jiang N, Zhang F, & Zhu W. (2023). Heat Stress Recovery of Chlorophyll Fluorescence in Tomato (*Lycopersicon esculentum* Mill.) Leaves through Nitrogen Levels. *Agronomy*, 13(12), 2858. <https://doi.org/10.3390/agronomy13122858>
- Marečková M, Barták M, & Hájek J. (2019). Temperature effects on photosynthetic performance of Antarctic lichen *Dermatocarpon polyphyllum*: A chlorophyll fluorescence study. *Polar Biology*, 42, 685–701. <https://doi.org/10.1007/s00300-019-02464-w>
- Mariem S, González-Torralba J, Collar C, Aranjuelo Í, & Morales F. (2020). Durum Wheat Grain Yield and Quality under Low and High Nitrogen Conditions: Insights into Natural Variation in Low- and High-Yielding Genotypes. *Plants*, 9(12), 1636. <https://doi.org/10.3390/plants9121636>

Investigación y Desarrollo (ANID), Fondecyt Regular Grant N°1211473. Proyecto VRID INT N°2023000997INT; UCO21102.

Data Availability Statement

Data are available upon request from E.O-G.

Acknowledgements

This work was supported by the project Fondecyt Iniciación N°11201086 and Fondecyt Regular N°1211473 from the Agencia Nacional de Investigación y Desarrollo–ANID. We thank Dr. Roke Rojas and Dr. Antonio Escandón for their technical support in physiological measurements.

Conflicts of Interest

The authors declare no conflict of interest. The funders had no role in the design of the study; in the collection, analyses, or interpretation of data; in the writing of the manuscript; or in the decision to publish the results.

Peer Review Statement

Plant Ecophysiology acknowledges the contributions of two anonymous reviewers to the peer review of this manuscript.

- Maxwell K, & Johnson GN. (2000). Chlorophyll fluorescence—A practical guide. *Journal of Experimental Botany*, 51(345), 659–668. <https://doi.org/10.1093/jexbot/51.345.659>
- Netshimbupfe M, Berner J, & Gouws C. (2022). The interactive effects of drought and heat stress on photosynthetic efficiency and biochemical defense mechanisms of Amaranthus species. *Plant-Environment Interactions*, 3(5), 212–225. <https://doi.org/10.1002/pei3.10092>
- Ostria-Gallardo E, Larama G, Berríos G, Fallard A, Gutiérrez-Moraga A, Ensminger I, Manque P, Bascañán-Godoy L, & Bravo LA. (2020). Decoding gene networks modules that explain the recovery of *Hymenoglossum cruentum* Cav. after extreme desiccation. *Frontiers in Plant Science*, 11, 574. <https://doi.org/10.3389/fpls.2020.00574>
- Palma JM, Jiménez A, Sandalio LM, Corpas FJ, Lundqvist M, Gomez M, & del Río LA. (2014). Antioxidative enzymes from chloroplasts, mitochondria, peroxisomes, and cytosol. *Plant Peroxisomes* in JM Palma, FJ Corpas, LA del Río (eds.), pp. 1–35. https://doi.org/10.1007/978-94-007-6889-5_12
- Pang Z, Lu Y, Zhou G, Hui F, Xu L, Viau C, & Xia J. (2024). MetaboAnalyst 6.0: Towards a unified platform for metabolomics data processing, analysis and interpretation. *Nucleic Acids Research*, 52(W1), W398–W406. <https://doi.org/10.1093/nar/gkae253>
- Peng J, Feng Y, Wang X, Li J, Xu G, Phonenasay S, Luo Q, Han Z, & Lu W. (2021). Effects of nitrogen application rate on the photosynthetic pigment, leaf fluorescence characteristics, and yield of indica hybrid rice and their interrelations. *Scientific Reports*, 11, 7485. <https://doi.org/10.1038/s41598-021-86858-z>
- Perera-Castro A, & Flexas J. (2023). The ratio of electron transport to assimilation (ETR/An): Underutilized but essential for assessing both equipment's proper performance and plant status. *Planta*, 257, 29. <https://doi.org/10.1007/s00425-022-04063-2>
- Plett D, Ranathunge K, Melino V, Kuya N, Uga Y, & Kronzucker H. (2020). The intersection of nitrogen nutrition and water use in plants: New paths toward improved crop productivity. *Journal of Experimental Botany*, 71(15), 4452–4468. <https://doi.org/10.1093/jxb/eraa049>
- Pollastrini M, Brüggeman W, Fotelli M, & Bussotti F. (2022). Downregulation of PSI regulates photosynthesis in early successional tree species. Evidence from a field survey across European forests. *Journal of Photochemistry and Photobiology*, 12, 100145. <https://doi.org/10.1016/j.jpap.2022.100145>
- Purcell LC, & King CA. (1996). Drought and nitrogen source effects on nitrogen nutrition, seed growth, and yield in soybean. *Journal of Plant Nutrition*, 19(6), 969–993. <https://doi.org/10.1080/01904169609365173>
- Ren B, Dong S, Zhao B, Liu P, & Zhang J. (2017). Responses of nitrogen metabolism, uptake and translocation of maize to waterlogging at different growth stages. *Frontiers in Plant Science*, 8, 1216. <https://doi.org/10.3389/fpls.2017.01216>
- Rice-Evans C, Miller N, & Paganga G. (1997) Antioxidant properties of phenolic compounds. *Trends in Plant Science*, 2(4), 152–159. [https://doi.org/10.1016/S1360-1385\(97\)01018-2](https://doi.org/10.1016/S1360-1385(97)01018-2)
- Sadak MS, & Ramadan AAEM. (2021). Impact of melatonin and tryptophan on water stress tolerance in white lupine (*Lupinus termis* L.). *Physiology and Molecular Biology of Plants*, 27, 469–481. <https://doi.org/10.1007/s12298-021-00958-8>
- Sadras VO, & Rodriguez D. (2010). Modelling the nitrogen-driven trade-off between nitrogen utilisation efficiency and water use efficiency of wheat in eastern Australia. *Field Crops Research*, 118(3), 297–305. <https://doi.org/10.1016/j.fcr.2010.06.010>
- Serôdio J, Schmidt W, & Frankenbach S. (2017). A chlorophyll fluorescence-based method for the integrated characterization of the photophysiological response to light stress. *Journal of Experimental Botany*, 68(5), 1123–1135. <https://doi.org/10.1093/jxb/erw492>
- Song Y, Li J, Liu M, Meng Z, Liu K, & Sui N. (2019a). Nitrogen increases drought tolerance in maize seedlings. *Functional Plant Biology*, 46(4), 350–359. <https://doi.org/10.1071/FP18186>
- Song X, Zhou G, Ma B, Wu W, Ahmad I, Zhu G, Yan W, & Jiao X. (2019b). Nitrogen Application Improved Photosynthetic Productivity, Chlorophyll Fluorescence, Yield and Yield Components of Two Oat Genotypes under Saline Conditions. *Agronomy*, 9(3), 115. <https://doi.org/10.3390/AGRONOMY9030115>
- Sumner L, Amberg A, Barrett D, Beale M, Beger R, Daykin C, Fan T, Fiehn O, Goodacre R, Griffin J, Hankemeier T, Hardy N, Harnly J, Higashi R, Kopka J, Lane A, Lindon J, Marriott P, Nicholls A, Reilly M, Thaden J, & Viant M. (2007). Proposed minimum reporting standards for chemical analysis. *Metabolomics*, 3, 211–221. <https://doi.org/10.1007/s11306-007-0082-2>
- Sun JY, Gao JL, & Lu XH. (2007). The effects of nitrogen on physiological indexes of drought tolerance and water use efficiency in soybean. *Soybean Science*. 26(4), 517–522.
- Tariq A, Pan K, Olatunji OA, Graciano C, Li N, Li Z, Song D, Sun F, Justine MF, Huang D, Gong S, Pandey B, Idrees M, & Dakhil MA. (2019). Role of nitrogen supplementation in alleviating drought-associated growth and metabolic impairments in Phoebe zhennan seedlings. *Journal of Plant Nutrition and Soil Science*, 182(4), 586–596. <https://doi.org/10.1002/jpln.201800435>
- The S, Snyder R, & Tegeder M. (2021). Targeting Nitrogen Metabolism and Transport Processes to Improve Plant Nitrogen Use Efficiency. *Frontiers in Plant Science*, 11. <https://doi.org/10.3389/fpls.2020.628366>
- Watanabe M, Balazadeh S, Toghe T, Erban A, Giavalisco P, Kopka J, Mueller-Roeber B, Fernie A, & Hoefgen R. (2013). Comprehensive dissection of spatiotemporal metabolic shifts in primary, secondary, and lipid metabolism during developmental senescence in Arabidopsis. *Plant Physiology*, 162(3), 1290–1310. <https://doi.org/10.1104/pp.113.217380>
- Wu Y, Li Q, Jin R, Chen W, Liu X, Kong F, Ke Y, Shi H, & Yuan J. (2019). Effect of low-nitrogen stress on photosynthesis and chlorophyll fluorescence characteristics of maize cultivars with different low-nitrogen tolerances. *Journal of Integrative Agriculture*, 18(6), 1246–1256. [https://doi.org/10.1016/S2095-3119\(18\)62030-1](https://doi.org/10.1016/S2095-3119(18)62030-1)
- Wu Y, Zhao B, Li Q, Kong F, Du L, Zhou F, Shi H, Ke Y, Liu Q, Feng D, & Yuan J. (2019). Non-structural carbohydrates in maize with different nitrogen tolerance are affected by nitrogen addition. *PLoS ONE*, 14, e0225753. <https://doi.org/10.1371/journal.pone.0225753>
- Zhao H, Sun S, Zhang L, Yang J, Wang Z, Ma F, & Li M. (2020). Carbohydrate metabolism and transport in apple roots under nitrogen deficiency. *Plant Physiology and Biochemistry*, 155, 455–463. <https://doi.org/10.1016/j.plaphy.2020.07.037>
- Zubillaga MF, Camina R, Orioli GA, & Barrio DA. (2019). Response of Amaranthus cruentus cv Mexicano to nitrogen fertilization under irrigation in the temperate, semiarid climate of North Patagonia, Argentina. *Journal of Plant Nutrition*, 42(2), 99–110. <https://doi.org/10.1080/01904167.2018.1549674>